Regulation of Shaoyao Ruangan Mixture on Intestinal Flora in Mice With Primary Liver Cancer

Hongde Zhen, MD[1,2,*] ⓘD, Xiang Qian, MD[2,*], Xiaoxuan Fu, MD[1],
Zhuo Chen, MD[1], Aiqin Zhang, PhD[2], and Lei Shi, MD[2]

Abstract

Background: Shaoyao Ruangan mixture (SRM) has been applied clinically for more than 20 years in Zhejiang Cancer Hospital to treat patients with primary liver cancer (PLC). Intestinal microecology plays an important role in the emergence of liver diseases. This study aimed to reveal connections among SRM, intestinal microbiota and PLC, and the potential targets of SRM for liver cancer. **Methods:** We established a control group, a PLC model group, and a treatment group of mice to analyze the inhibitory effect of SRM on PLC and its intestinal flora target. We also evaluated drug efficacy of SRM and analyzed specific changes in intestinal flora by 16S rDNA sequencing of stools. As the serum interleukin (IL)-10 level could be an independent prognostic factor for unresectable liver cancer, we detected IL-10 levels and analyzed their association with the abundance of specific bacteria. **Results:** Liver tumors in the treatment group were smaller and fewer than those in the model group (*P* = .046). The abundance of *Bacteroides* was significantly higher in the model group than that in the control group, while SRM significantly reduced the increasing abundance of *Bacteroides* in mice with PLC. We found that the IL-10 level was positively correlated with the abundance of *Bacteroides*. **Conclusion:** SRM can effectively inhibit the progression of PLC and increase *Bacteroides* abundance. In view of the association between *Bacteroides* and liver cancer and the significant positive correlation between *Bacteroides* and IL-10 levels, *Bacteroides* may be the target intestinal flora of SRM to inhibit PLC.

Introduction

Approximately half of all new cases of primary liver cancer (PLC) and associated deaths worldwide occur in China.[1] Due to an insufficient understanding of drug mechanisms and targets, a large number of clinical trials fail.[2-4] The adaptability and stability of intestinal microbiota and their responsiveness to physiological and pathological changes make them possible biomarkers and therapeutic targets for tumors.[5] Further exploration of intestinal microbiota promotes an understanding of the pathogenesis and prevention of hepatocellular carcinoma (HCC).[6] For example, intestinal bacterial metabolites engage key pathways to promote inflammation, fibrosis, and genotoxicity in HCC; and a tumor-promoting microenvironment caused by gram-positive intestinal flora promotes the development of HCC.[7,8] Traditional Chinese medicine (TCM) is one of the oldest medical systems in the world and has been used in China for thousands of years.[9,10] The TCM preparation Shaoyao Ruangan mixture (SRM) made by Zhejiang Cancer Hospital has been applied clinically for

[1]Second Clinical Medical College, Zhejiang Chinese Medical University, Hangzhou, People's Republic of China
[2]Zhejiang Cancer Hospital, Hangzhou, People's Republic of China

*Hongde Zhen and Xiang Qian contributed equally to this work.

Corresponding Author:
Lei Shi, Department of Mammary Oncology, Zhejiang Cancer Hospital, No. 1 East Banshan Road, Gongshu District, Hangzhou 310022, People's Republic of China.
Email: 13735520087@163.com

more than 20 years.[11] A case series reported that SRM may improve the survival and quality of life of patients with advanced liver cancer.[12] This study aimed to investigate the inhibitory effect of SRM on PLC in mice and the regulation of specific intestinal microbiota in order to explore its target intestinal flora.

Materials and Methods

Preparation of SRM

Shaoyao Ruangan mixture is a medical preparation formulated by the Hangzhou Traditional Chinese Medicine Hospital under medicine preparation Approval Number Z20100018. The batch number of the preparation used in this experiment is 160624. SRM consists of the following Chinese herbal medicinals[13]: Herba Hedyotidis (herb of *Hedyotis diffusa Willd*., Family Rubiaceae), 86 g; Scutellariae Barbatae Herba (herb of *Scutellaria barbata* D, Don, Family Lamiaceae), 86 g; Paridis Rhizoma (rhizomes of *Paris polyphylla* Smith var. *yunnanensis* [Franch.] Hand.-Mazz., Family Liliaceae), 28.7 g; Tetrastigma hemsleyanum Diels et Gilg (root of *Tetrastigma hemsleyanum* Diels et Gilg, FamilyVitaceaae), 34.4 g; Paeoniae Radix Alba (root of *Paeonia lactiflora* Pall, Family Ranunculaceae), 34.4 g; Galli Gigerii Endothelium Corneum (inside the gizzard of *Gallus gallus domesticus* Brisson, Family Phasianidae), 25.8 g; Citri Reticulatae Pericarpium Viride (immature peel of *Citrus reticulata* Blanco, Family Rutaceae), 25.8 g; Citri Reticulatae Pericarpium (ripe peel of *Citrus reticulata* Blanco, Family Rutaceae), 25.8 g; Crataegi Fructus (ripe fruit of *Crataegus pinnatifida* Bge, Family Rosaceae), 86 g; Curcumae Radix (root of *Curcuma wenyujin* Y. H. Chen et C. Ling., Family Zingiberaceae), 25.8 g; Sparganii Rhizoma (tuber of *Sparganium stoloniferum* Buch.-Ham., Family Sparganiaceae), 25.8 g; Curcumae Rhizoma (rhizomes of *Curcuma phaeocaulis* Val., Family Zingiberaceae), 25.8 g; Imperatae Rhizoma (rhizomes of *Imperata cylindrica* Beauv. var. *major* [Nees] C. E. Hubb., Family Gramineae), 86 g; Gardeniae Fructus Praeparatus (ripe fruit of *Gardenia jasminoides* Ellis, Family Rubiaceae), 25.8 g; Lysimachiae Herba (herb of *Lysimachia christinae* Hance, Family Primulaaceae), 86 g; Ardisiae Japonicae Herba (herb of *Ardisia japonica* [Thunb.] Blume, Family Myrsinaceae, Nom. Conserv.), 86 g; Aristolochia mollissima Hance (herb of *Aristolochia mollissima* Hance, Family Aristolochiaceae), 86 g; Liquidambaris Fructus (ripe infructescence of *Liquidambar formosana* Hance, Family Hamamelidaceae), 34.4 g; and Agrimoniae Herba (ground part of *Agrimonia pilosa* Ledeb., Family Rosaceae), 86 g. The above-mentioned 19 Chinese herbal medicines were boiled twice with water, the first decoction for 120 minutes and the second decoction for 90 minutes. After filtration, the 2 decoctions were combined and precipitated. The supernatant was aspirated and concentrated to 1000 mL. Then, it was packed, sealed, and steam-sterilized.

Transgenic PLC Model and Groups

Mutation of the Ras proto-oncogene or activation of the Ras signaling pathway is an essential feature of liver cancer.[14] The mechanism of Ras transformation in mice may differ from that in humans.[15] There are 3 Ras family genes related to human cancer: H-Ras, K-Ras, and N-Ras. H-Ras12V has a higher transforming potential than either K-Ras12V or N-Ras12V in RIE-1 rat epithelial cell cultures.[16] In 2005, Wang used a serum albumin enhancer and promoter to induce the specific expression of a mutant Ras oncogene (H-Ras12V) in hepatocytes and successfully established a mouse model of H-Ras12V transgenic liver cancer.[17]

The experiment included a control group, a model group, and a treatment group. Twenty-six 7-month-old SPF H-Ras12V transgenic male mice, established by Wang, were randomly assigned to the model group or the treatment group. These mice carried the H-Ras12V oncogene in the C57BL/6J genetic background. All mice weighed between 23.06 g and 31.00 g. The control group included 13 C57BL/6J male mice with weights ranging from 24.78 g to 34.61 g. The above-mentioned animals were bred and raised at the Experimental Animal Center of Dalian Medical University (Qualification No. 211003700000627). All mice were given a standard diet. Procedures involving animals and their care were conducted in conformity with the National Institutes of Health (NIH) guidelines (NIH Publication No. 85-23, revised 1996) and were approved by the Animal Care and Use Committee of the Zhejiang Cancer Hospital.

Treatment of PLC Mice

The mice in the treatment group were intragastrically administered 20 mg/kg body weight SRM decoction daily, while the mice in the control and model groups were intragastrically administered 20 mg/kg physiological saline every day. The entire treatment period lasted 12 weeks. The weight of each mouse was recorded once a week.

Model Assessment and Efficacy Evaluation

The model was assessed based on the general conditions of the mice and the liver tumor formation rate. The efficacy of SRM was evaluated by the following 2 aspects: (1) the general conditions of the mice, including fur condition, weight trend, and activity; and (2) the tumor characteristics, especially the size and number of liver tumors. Mice were sacrificed and dissected in the 12th week of the experiment. The diameter and number of liver tumors were recorded.

Determination of Serum Interleukin (IL)-10 Levels

The IL-10 test kit was used to detect serum IL-10 levels. After preparing all the reagents and standards, 50 μL sample diluent was added to each well. Within 15 minutes, 50 μL each of standards, samples, and controls were added to previously defined wells. Then, 50 μL detection antibody was added to each well. The antibodies were incubated for 3 hours at room temperature, and then, the plates were washed 6 times. After 45 minutes of incubation at room temperature, they were washed 6 times again. Then, 100 μL chromogenic substrate was added, and the plates were protected from light and incubated for 15 minutes at room temperature. Finally, 100 μL stop solution was added to each well. Within 30 minutes, the optical density was detected at a wavelength of 450 nm, with a reference wavelength of 570 nm or 630 nm.

Collection and Pretreatment of Intestinal Flora Samples

The stools of 7 randomly selected mice in each group were collected using sterile tweezers in the eighth week of the experiment. After swirling 0.1 g fecal specimens and 4 mL sterile phosphate-buffered saline (PBS; pH 7.4) for 5 minutes, each fecal specimen was centrifuged at $40\times g$ for 8 minutes. The upper layers containing bacteria were collected. The swirling and centrifugation steps were repeated once. The supernatants were collected and centrifuged at $2000\times g$ for 8 minutes. The obtained bacterial pellets were washed twice with PBS. Finally, the samples were stored in sterile EP tubes containing PBS at $-80°C$.

Sequencing of Intestinal Flora

Total DNA quality tests were performed by using a Thermo NanoDrop 2000 Ultraviolet Microspectrophotometer (Thermo Fisher Scientific Ltd.) and 1% agarose gel electrophoresis. The V3-V4 region of 16S rDNA was selected for amplification. The universal primers used were F341 and R806. The 5′ end of the universal primer was designed with the index sequence and linker sequence suitable for HiSeq 2500 PE250 sequencing: forward primer (5′-3′): ACTCCTACGGGRSGCAGCAG (F341); reverse primer (5′-3′): GGACTACVVGGGTATCTAATC (R806). To ensure the accuracy and efficiency of the amplification, polymerase chain reaction (PCR) was performed using the KAPA HiFi HotStart ReadyMix PCR kit (Sopachem Ltd.). The diluted genomic DNA served as a template. The PCR products were detected by 2% agarose gel electrophoresis and recovered by an AxyPrep DNA Gel Recovery Kit (Axygen Ltd.). Then, the library was examined by a Thermo NanoDrop 2000 Ultraviolet Microspectrophotometer and 2% agarose gel electrophoresis. After the quality of the library was confirmed, Qubit was used for library quantification. According to the quantity requirement for each sample, the appropriate amount of each reagent was mixed together. Finally, sequencing was performed using Illumina HiSeq PE250.

Processing of the Intestinal Flora Data

After quality control of the original data, reads were sorted by abundance from large to small. The operational taxonomic unit (OTU) was obtained by using USEARCH software to cluster the data with a standard of 97% similarity. Using QIIME software for alpha diversity analysis, the leveling parameters were determined. Then, 25 828 reads were randomly selected from each sample. A read was separately extracted from an OTU as the representative sequence. Using the Ribosomal Database Project classifier, the representative sequence was compared with the 16S database to perform taxa classification for each OTU. After classification, the OTU abundance table was made according to the number of sequences in each OTU. From this table, taxa abundance analysis, alpha diversity analysis, beta diversity analysis, and significant difference taxa analysis were performed.

Statistical Analysis

General Conditions of Mice and Tumor Characteristics. Measurement data are expressed as the mean and standard deviation ($\overline{x} \pm s$). Data with a normal distribution were compared with the independent sample *t* test. Repeated measurement data were analyzed by analysis of variance. Statistical analysis of ordered grade data was weighted on the basis of the number and conducted by the Mann-Whitney test. Statistical analysis was completed by SPSS statistical software V 23.0 (SPSS, Chicago, IL). *P* value <.05 was considered statistically significant.

Intestinal Microbiota. Differences in taxa communities among samples were compared by the UniFrac distance distribution. Analysis of significantly different taxa was performed by using linear discriminant analysis Effect Size (LEfSe analysis). The Kruskal-Wallis test was used to identify genera with significant differences ($P < .05$) among groups. The top 30 taxa in terms of abundance at the genus level were selected, and the Spearman correlation test was used to analyze the relationships among the dominant taxa. The correlation between serum IL-10 levels and *Bacteroides* was analyzed by Pearson correlation.

Results

Model Assessment and Drug Efficacy Evaluation

General Animal Conditions. The mice in the control group were the most active and responsive. Meanwhile, they had glossier fur. The mice suffering from PLC had messier fur
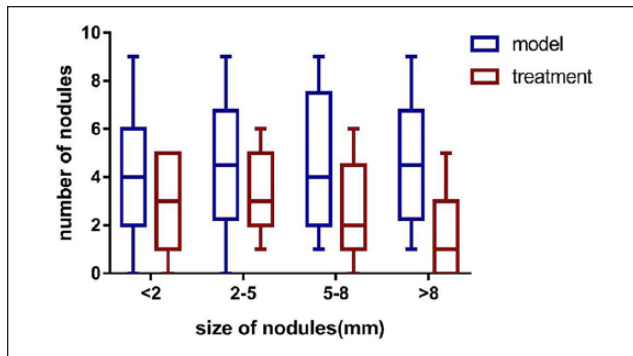
Figure 1. Size and number of tumors in the model group and the treatment group. After weighing the case by number, a Mann-Whitney test was performed ($Z = -2.032$, $P = .042$).

and slower responses. In the treatment group, the mice's fur became smoother and they reacted more sensitively to their circumstances.

Tumor Characteristics. Multiple tumors appeared in the liver of mice in the model group and the treatment group. The longest diameter of the largest tumor in the model group was 11.80 ± 5.01 mm. The longest diameter of the largest tumor in the treatment group was 10.91 ± 3.60 mm. Liver tumors in the 2 groups were classified into 4 categories of <2 mm, 2 to 5 mm, 5 to 8 mm, and >8 mm. Tumors in the treatment group were fewer in number and smaller than those in the model group. As shown in Figure 1, there was a significant inhibitory effect of SRM on liver cancer development in mice.

Changes in Body Weight Over Time. The body weight of mice in the control group showed a continuous and steady increase. The body weight of mice in the model group showed a slightly curved trend, first increasing and then gradually stabilizing before finally showing a downward trend. The body weight of mice in the treatment group was stable from beginning to end. The weight trend over time of each group is shown in Figure 2 as $\bar{x} \pm s$. The difference in the body weight of mice in different groups was not statistically significant, but the difference in body weight over time was statistically significant. In addition, there was an interaction effect between mouse body weight and time in different groups. This finding indicated that SRM could maintain stable body weight with the progression of PLC.

Taxa Abundance Analysis

According to the taxa annotation results, the taxa abundance of each group was analyzed at the genus level. The top 5 genera with the highest abundance in the control group were
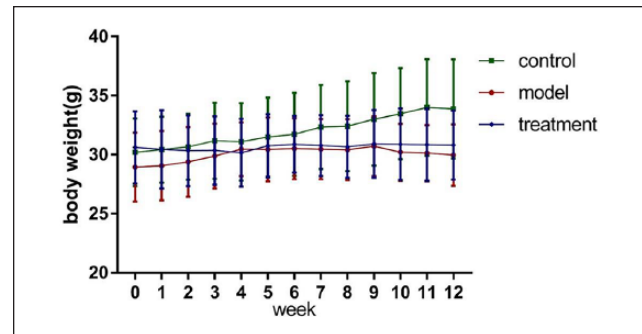

Figure 2. The body weight of the mice changed over time. Analysis of variance of repeated measurement data was used to examine the effects of time and group on mouse body weight and their interactions. The corrected intrasubject effect (time) was statistically significant ($P = .003$). The intersubject effect (group) test had a P value of .232, and there was no significant difference in mouse body weight in different groups. The interaction effect analysis revealed an interaction between group and time, which meant that group allocation influenced the trend in mouse body weight over time ($P = .039$).

Alloprevotella, Barnesiella, Clostridium XlVa, Bacteroides, and *Alistipes*. The top 5 genera in the model group with the highest abundance were *Barnesiella, Alloprevotella, Bacteroides, Clostridium XlVa*, and *Saccharibacteria genus incertae sedis*. Correspondingly, *Barnesiella, Desulfovibrio, Clostridium XlVa, Saccharibacteria genus incertae sedis*, and *Bacteroides* were the top 5 dominant taxa in the treatment group. The abundance of taxa and their proportions in the 3 groups are shown in Figure 3.

Analysis of Taxa With Significant Differences in Abundance

As shown in Figure 4A, the different genera between the control group and the model group were *Bacteroides, Saccharibacteria genera incertae sedis, Parabacteroides, Flavonifractor, Akkermansia*, and *Allobaculum*. The different genera between the model group and the treatment group were *Alloprevotella, Bacteroides, Desulfovibrio, Turicibacter*, and *Clostridium XVIII*, and more details can be found in Figure 4B. The abundance of *Bacteroides* increased significantly in mice with liver cancer and decreased after treatment with SRM. These important data can be seen in Figure 4C.

Correlation Between Serum IL-10 Level and Bacteroides Abundance

In these 3 groups of mice, the level of IL-10 was positively correlated with the abundance of *Bacteroides*, and the Pearson correlation test showed that this correlation was statistically significant (Figure 5).
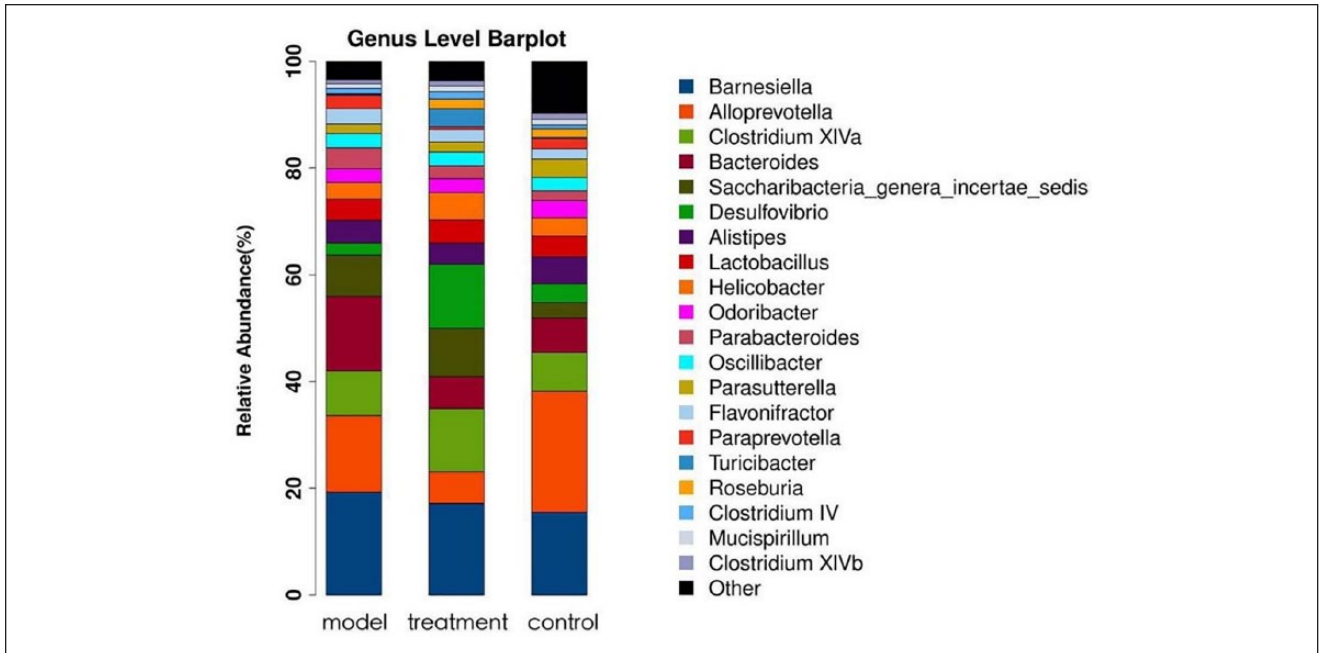
Figure 3. Taxa abundance histogram at the genus level.
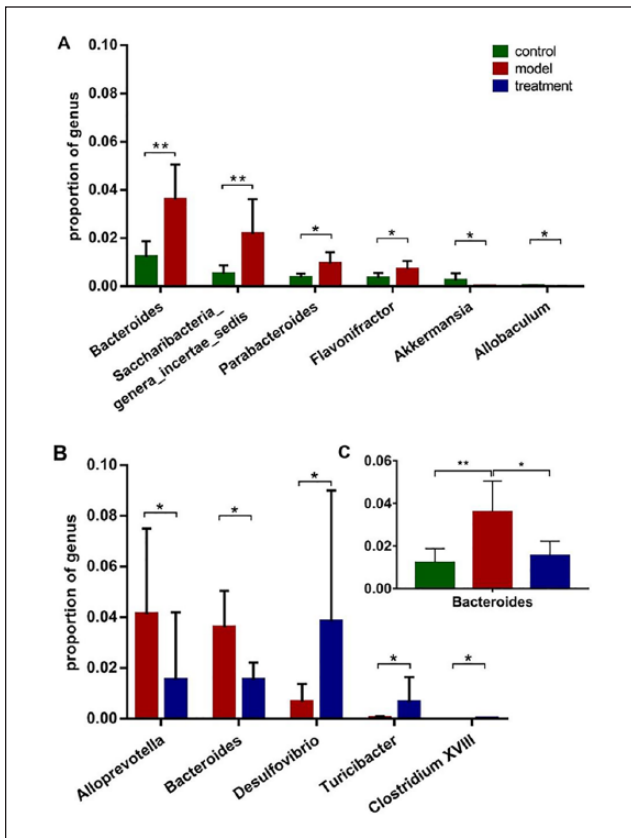

Figure 4. Significantly different taxa at the genus level. The Kruskal-Wallis test was used to identify taxa with significant differences between groups ($P < .05$). *$P < .05$, **$P < .01$.
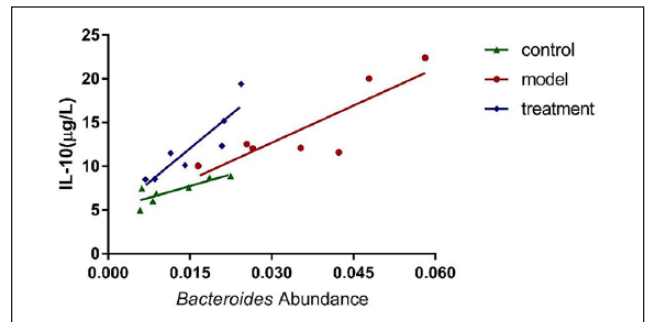

Figure 5. A scatter plot of serum interleukin (IL)-10 levels and *Bacteroides* abundance. The Pearson correlation coefficient was 0.837 ($P < .05$) in the control group, 0.856 ($P < .05$) in the model group, and 0.898 ($P < .01$) in the treatment group.

Spearman Correlation of Dominant Taxa

The top 30 genera with differential abundance were selected to explore the relationships among the dominant taxa. The Spearman correlation heat map was drawn by the corrplot package in R software. The important patterns and relationships among the dominant taxa were analyzed using this heat map. The Spearman correlation analysis between the control group and the model group is shown in Figure 6A. Taking $P < .01$ as the level of significance, there were significant positive correlations between *Bacteroides* and *Parabacteroides* and between *Akkermansia* and *Escherichia*. There were significant negative correlations between *Bacteroides* and *Allobaculum, Akkermansia* and
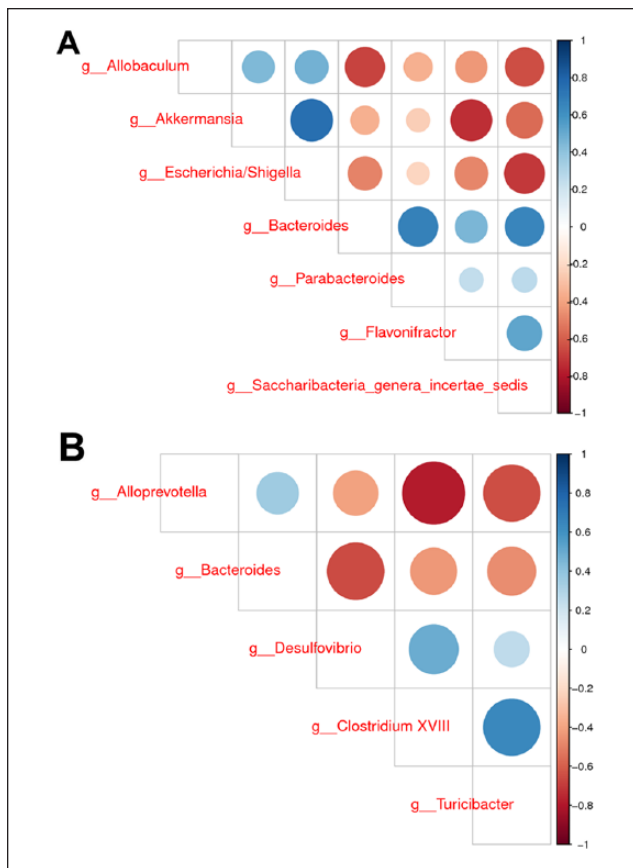
Figure 6. (A) Spearman correlation analysis of the control group and the model group. (B) Spearman correlation analysis of the model group and the treatment group. Blue indicates a positive correlation, and red indicates a negative correlation. A darker color indicates a stronger correlation between taxa.

Flavonifractor, and *Escherichia* and *Saccharibacteria genus incertae sedis*. Taking $P < .05$ as the level of significance, there were significant negative correlations between *Alloprevotella* and *Clostridium XVIII, Alloprevotella* and *Turicibacter*, and *Bacteroides* and *Desulfovibrio*, and there was a positive correlation between *Clostridium XVIII* and *Turicibacter*. The Spearman correlation analysis of the model group and the treatment group is shown in Figure 6B.

Discussion

Potential Intestinal Flora Target of SRM

Differences in intestinal flora are an important factor in tumor immunotherapy.[18] The activity of antitumor drugs relates to the type of bacteria that live in the human intestinal tract.[19] This study found that the intestinal microbiota of SRM-treated mice with liver cancer underwent specific changes. The abundance of *Bacteroides* in the model group increased significantly compared with that in the control

group, while the abundance of *Bacteroides* in the treatment group decreased significantly compared with that in the model group.

Bacteroides is 1 of the 3 major intestinal genera in the human body.[20] The abundance of *Bacteroides* in the intestine increases significantly when people keep a high-fat and high-protein diet for a long period.[21] Sphingolipid is a common feature of *Bacteroides* and an important factor in the ability of these organisms to become dominant bacteria in the intestine.[22] Sphingolipids regulate multiple cellular processes, including proliferation, cell cycle, inflammatory pathways, and apoptosis. Some sphingolipids have opposing functions, and their metabolic dysfunction can lead to the loss of cell cycle control.[23] For example, the sphingolipid metabolite ceramide can regulate cell proliferation, differentiation, and apoptosis; reverse drug resistance; and inhibit tumors.[24] Studies have shown that *Bacteroides fragilis* of the genus *Bacteroides* is more abundant in patients with colorectal cancer than in healthy individuals and that *Bacteroides fragilis* causes carcinogenesis of the colon.[25,26] In addition to the genus *Bacteroides*, the genera *Porphyromonas* and *Prevotella* also have sphingolipids.[22] *Porphyromonas gingivalis* of the genus *Porphyromonas* is an oral microbe that causes periodontitis and is associated with various tumors, such as colorectal cancer, non-Hodgkin's lymphoma, oral cavity cancer, gastrointestinal cancer, and pancreatic cancer.[27,28] However, *Prevotella* has exactly the opposite clinical value. An increase in *Prevotella* abundance can promote the release of anti-inflammatory substances and ultimately inhibit liver cancer.[29] In conclusion, the unique structure of *Bacteroides* and its metabolites are closely related to liver cancer and other types of cancer.

SRM consists of 19 Chinese herbal medicinals. There are no reports of the effects of these medicinals on intestinal flora in animals or humans. Some researchers previously analyzed the arbuscular mycorrhizal fungi of *Poncirus trifoliata* and *Citrus reticulata* by SSU rDNA analysis, and 5 strains isolated from citrus orchards promote the early emergence and growth of citrus seedlings.[30,31] Another study found a high potential for the application of *Streptomyces violascens* MT7, an Indian indigenous, Loktak Lake soil isolate, and its extracellular metabolites as an effective eco-friendly alternative to synthetic fungicides for controlling toxigenic citrus and papaya-rotting fungi.[32] However, there is no evidence to suggest that these Chinese herbal medicinals are linked to intestinal microecology.

Other Changes in Intestinal Flora in the Context of Liver Cancer

In addition to the significant increase in the abundance of *Bacteroides*, this study also found that the abundance of *Akkermansia* significantly decreased in mice with liver

cancer. The abundance of *Akkermansia* is inversely related to mouse body weight, which contrasts the positive correlation of *Bacteroides* with high-fat and high-protein diets.[33] Recent studies have shown that *Akkermansia muciniphila* can improve immunotherapy for epithelial-derived tumors.[34] Therefore, the correlation between liver cancer and *Akkermansia* still needs further exploration.

Allobaculum is another intestinal flora that is negatively related to mouse body weight.[33] This study found a negative correlation between *Allobaculum* and *Bacteroides*. As obesity and a diet high in animal fat can increase the risk of liver cancer, the abundance of *Allobaculum* and the ratio of *Allobaculum* to *Bacteroides* in the pathogenesis of liver cancer require further study.[35]

Correlation Between IL-10 Levels and *Bacteroides* Abundance

Serum IL-10 is closely related to PLC. It is not only a complementary tumor marker for patients with low α-fetoprotein levels but also an independent prognostic factor for unresectable HCC.[36,37] Increased IL-10 production accelerates the progression of chronic hepatitis B virus infection and the development of HCC.[38] A study assessing the association between the IL-10 polymorphisms IL-10-1082 (G/A), IL-10-592 (C/A), IL-10-819 (T/C), and HCC susceptibility found that the IL-10-592 A/C polymorphism may be associated with HCC among Asians.[39] Therefore, we evaluated IL-10 in mice with liver cancer.

Previous studies have found that IL-10 levels are positively correlated with the abundance of *Bacteroides fragilis*.[40] For example, *Bacteroides fragilis* could inhibit colitis by responding to IL-10 produced by $CD4^+$ T-cells.[41] Further studies found that *Bacteroides fragilis* protected against colitis induced by *Helicobacter hepaticus* by promoting IL-10 production by CD4+ T-cells.[42] There was a significant positive correlation between IL-10 level and *Bacteroides* abundance in this study. On the one hand, *Bacteroides* abundance and serum IL-10 levels were significantly increased in mice with liver cancer compared with normal mice, which indicated their potential as auxiliary diagnostic markers. On the other hand, the abundance of *Bacteroides* specifically decreased after treatment with SRM. SRM plays a role in prolonging the survival time of patients with liver cancer, and the abundance of *Bacteroides* may also be an independent prognostic factor for liver cancer.

Conclusions

SRM could effectively inhibit the progression of tumors in mice with PLC and regulate their intestinal microecology. *Bacteroides* was regarded as the potential intestinal flora target of SRM. However, intestinal microecology is very complex and can adapt to many factors, such as diet, environment, physiology, and pathological conditions.[5] Studying these adaptations requires systematic and complex evaluation methods. The existing research methods focus on intestinal flora diversity, bacterial structure, and differential species abundance; and 2×2 correlation analyses of differences in species and dominant species can be performed. However, the changes in intestinal microecology influence the relationships among many bacterial communities, which form a very complex network, and further improvement in microecological evaluation methods is required. The composition of compound TCM formulas is complex, so its mechanism of treating disease is difficult to fully clarify. Because of its systemic effects and complexity, intestinal microecology is a valuable system to evaluate when studying the antitumor mechanism of compound TCM formulas.

ORCID iD

Hongde Zhen https://orcid.org/0000-0002-1917-3871

References

1. Torre LA, Bray F, Siegel RL, Ferlay J, Lortet-Tieulent J, Jemal A. Global cancer statistics, 2012. *CA Cancer J Clin*. 2015;65:87-108.

2. Gerbes A, Zoulim F, Tilg H, et al. Gut roundtable meeting paper: selected recent advances in hepatocellular carcinoma. *Gut*. 2018;67:380-388.

3. Bruix J, Gores GJ, Mazzaferro V. Hepatocellular carcinoma: clinical frontiers and perspectives. *Gut*. 2014;63:844-855.

4. Bruix J, Reig M, Sherman M. Evidence-based diagnosis, staging, and treatment of patients with hepatocellular carcinoma. *Gastroenterology*. 2016;150:835-853.

5. Cammarota G, Ianiro G. Gut microbiota and cancer patients: a broad-ranging relationship. *Mayo Clin Proc*. 2017;92:1605-1607.

6. Brandi G, De Lorenzo S, Candela M, et al. Microbiota, NASH, HCC and the potential role of probiotics. *Carcinogenesis*. 2017;38:231-240.

7. Yu LX, Schwabe RF. The gut microbiome and liver cancer: mechanisms and clinical translation. *Nat Rev Gastroenterol Hepatol*. 2017;14:527-539.

8. Loo TM, Kamachi F, Watanabe Y, et al. Gut microbiota promotes obesity-associated liver cancer through PGE2-mediated suppression of antitumor immunity. *Cancer Discov*. 2017;7:522-538.

9. Stone R. Biochemistry. Lifting the veil on traditional Chinese medicine. *Science*. 2008;319:709-710.

10. Tang JL, Liu BY, Ma KW. Traditional Chinese medicine. *Lancet*. 2008;372:1938-1940.

11. He F, Zhong H. Treating 21 cases of chemotherapy liver damage with Shaoyao Ruangan mixture. *Zhejiang Cancer*. 1998;4:131.

12. Gong L, Jiang C. Treating 58 cases of advanced primary liver cancer with Shaoyao Ruangan mixture. *Chin J Integr Tradit Chin West Med*. 2005;25:848-849.

13. Wang Q, Wang C, Hou G. Preparation and clinical application of Shaoyao Ruangan mixture. *Jiangxi J Tradit Chin Med*. 2006;37:51-52.

14. Pang RW, Poon RT. From molecular biology to targeted therapies for hepatocellular carcinoma: the future is now. *Oncology*. 2007;72(suppl 1):30-44.

15. Hamad NM, Elconin JH, Karnoub AE, et al. Distinct requirements for Ras oncogenesis in human versus mouse cells. *Genes Dev*. 2002;16:2045-2057.

16. Li W, Zhu T, Guan KL. Transformation potential of Ras isoforms correlates with activation of phosphatidylinositol 3-kinase but not ERK. *J Biol Chem*. 2004;279:37398-37406.

17. Wang AG, Moon HB, Lee MR, et al. Gender-dependent hepatic alterations in H-ras12V transgenic mice. *J Hepatol*. 2005;43:836-844.

18. Gopalakrishnan V, Spencer CN, Nezi L, et al. Gut microbiome modulates response to anti-PD-1 immunotherapy in melanoma patients. *Science*. 2018;359:97-103.

19. Scott TA, Quintaneiro LM, Norvaisas P, et al. Host-microbe co-metabolism dictates cancer drug efficacy in *C. elegans. Cell*. 2017;169:442-456.e18.

20. Arumugam M, Raes J, Pelletier E, et al. Enterotypes of the human gut microbiome. *Nature*. 2011;473:174-180.

21. Wu GD, Chen J, Hoffmann C, et al. Linking long-term dietary patterns with gut microbial enterotypes. *Science*. 2011;334:105-108.

22. Kato M, Muto Y, Tanaka-Bandoh K, Watanabe K, Ueno K. Sphingolipid composition in *Bacteroides* species. *Anaerobe*. 1995;1:135-139.

23. Patwardhan GA, Beverly LJ, Siskind LJ. Sphingolipids and mitochondrial apoptosis. *J Bioenerg Biomembr*. 2016;48:153-168.

24. Li F, Zhang N. Ceramide: therapeutic potential in combination therapy for cancer treatment. *Curr Drug Metab*. 2015;17:37-51.

25. Sears CL, Geis AL, Housseau F. *Bacteroides fragilis* subverts mucosal biology: from symbiont to colon carcinogenesis. *J Clin Invest*. 2014;124:4166-4172.

26. Toprak NU, Yagci A, Gulluoglu BM, et al. A possible role of *Bacteroides fragilis* enterotoxin in the aetiology of colorectal cancer. *Clin Microbiol Infect*. 2006;12:782-786.

27. Atanasova KR, Yilmaz O. Looking in the *Porphyromonas gingivalis* cabinet of curiosities: the microbium, the host and cancer association. *Mol Oral Microbiol*. 2014;29:55-66.

28. Barton MK. Evidence accumulates indicating periodontal disease as a risk factor for colorectal cancer or lymphoma. *CA Cancer J Clin*. 2017;67:173-174.

29. Li J, Sung CY, Lee N, et al. Probiotics modulated gut microbiota suppresses hepatocellular carcinoma growth in mice. *Proc Natl Acad Sci U S A*. 2016;113:E1306-E1315.

30. Wang P, Wang Y. Community analysis of arbuscular mycorrhizal fungi in roots of *Poncirus trifoliata* and *Citrus reticulata* based on SSU rDNA. *ScientificWorldJournal*. 2014;2014:562797.

31. Thokchom E, Kalita MC, Talukdar NC. Isolation, screening, characterization, and selection of superior rhizobacterial strains as bioinoculants for seedling emergence and growth promotion of Mandarin orange (*Citrus reticulata* Blanco). *Can J Microbiol*. 2014;60:85-92.

32. Choudhary B, Nagpure A, Gupta RK. Biological control of toxigenic citrus and papaya-rotting fungi by *Streptomyces violascens* MT7 and its extracellular metabolites. *J Basic Microbiol*. 2015;55:1343-1356.

33. Baldwin J, Collins B, Wolf PG, et al. Table grape consumption reduces adiposity and markers of hepatic lipogenesis and alters gut microbiota in butter fat-fed mice. *J Nutr Biochem*. 2016;27:123-135.

34. Routy B, Le Chatelier E, Derosa L, et al. Gut microbiome influences efficacy of PD-1-based immunotherapy against epithelial tumors. *Science*. 2018;359:91-97.

35. Freedman ND, Cross AJ, McGlynn KA, et al. Association of meat and fat intake with liver disease and hepatocellular carcinoma in the NIH-AARP cohort. *J Natl Cancer Inst*. 2010;102:1354-1365.

36. Hsia CY, Huo TI, Chiang SY, et al. Evaluation of interleukin-6, interleukin-10 and human hepatocyte growth factor as tumor markers for hepatocellular carcinoma. *Eur J Surg Oncol*. 2007;33:208-212.

37. Chan SL, Mo FK, Wong CS, et al. A study of circulating interleukin 10 in prognostication of unresectable hepatocellular carcinoma. *Cancer*. 2012;118:3984-3992.

38. Shin HD, Park BL, Kim LH, et al. Interleukin 10 haplotype associated with increased risk of hepatocellular carcinoma. *Hum Mol Genet*. 2003;12:901-906.

39. Wei YG, Liu F, Li B, et al. Interleukin-10 gene polymorphisms and hepatocellular carcinoma susceptibility: a meta-analysis. *World J Gastroenterol*. 2011;17:3941-3947.

40. Round JL, Mazmanian SK. Inducible Foxp3+ regulatory T-cell development by a commensal bacterium of the intestinal microbiota. *Proc Natl Acad Sci U S A*. 2010;107:12204-12209.

41. Cohen-Poradosu R, McLoughlin RM, Lee JC, Kasper DL. *Bacteroides fragilis*–stimulated interleukin-10 contains expanding disease. *J Infect Dis*. 2011;204:363-371.

42. Mazmanian SK, Round JL, Kasper DL. A microbial symbiosis factor prevents intestinal inflammatory disease. *Nature*. 2008;453:620-625.